# A Low-Complexity Analytical Modeling for Cross-Layer Adaptive Error Protection in Video Over WLAN

Hossein Bobarshad, *Graduate Student Member, IEEE*, Mihaela van der Schaar, *Fellow, IEEE*, and Mohammad R. Shikh-Bahaei, *Senior Member, IEEE*

***Abstract*—We find a low-complicity and accurate model to solve the problem of optimizing MAC-layer transmission of real-time video over wireless local area networks (WLANs) using cross-layer techniques. The objective in this problem is to obtain the optimal MAC retry limit in order to minimize the total packet loss rate. First, the accuracy of Fluid and M/M/1/K analytical models is examined. Then we derive a closed-form expression for service time in WLAN MAC transmission, and will use this in mathematical formulation of our optimization problem based on M/G/1 model. Subsequently we introduce an approximate and simple formula for MAC-layer service time, which leads to the M/M/1 model. Compared with M/G/1, we particularly show that our M/M/1-based model provides a low-complexity and yet quite accurate means for analyzing MAC transmission process in WLAN. Using our M/M/1 model-based analysis, we derive closed-form formulas for the packet overflow drop rate and optimum retry-limit. These closed-form expressions can be effectively invoked for analyzing adaptive retry-limit algorithms. Simulation results (network simulator-2) will verify the accuracy of our analytical models.**

***Index Terms*—Cross-layer, IEEE-WLAN, queuing system, retransmission, retry-limit.**

## I. Introduction

THE IEEE Wireless Local Area Network (WLAN) [2] is the most common technology for indoor broadband wireless access. However it does not guarantee quality-of-service (QoS) for many of the present and forthcoming multimedia applications, such as video chat, Multimedia Messaging Service (MMS), high definition TV content, mobile TV, and Digital Video Broadcasting (DVB).

Cross-layer strategies have lately attracted particular attention for QoS improvement over WLANs (for instance, see [3]–[7] and [8]). QoS for video transmission over WLAN networks has been studied in [3], wherein a priority queuing mechanism at the network layer in conjunction with retry-limit adaptation in the MAC layer is employed. The aim in [3] is to derive the optimum retry-limit in order to minimize the "total packet loss rate", which encompasses only the "packet link loss rate" and "packet overflow drop rate". An overview of cross-layer schemes for improving multimedia transmission over wireless LANs is provided in [9]. Since the review work in [9], the cross-layer optimization techniques have progressed extensively in the area of wireless communications. In [10], an optimization technique is studied by considering network layer and MAC layer in order to improve the QoS over IEEE WLANs. Authors in [11] illustrate a simple cross-layer strategy using prioritized video frame at the Application (APP) layer, frame length and retry-limit at the MAC layer, and modulation schemes at the Physical (PHY) layer to improve the quality of multimedia. They did not provide analytical solution for the optimal retry-limit; nevertheless, they evaluated the optimal retry-limit for some sample video sequences using simulations. A cross-layer design for reliable video transmission over wireless ad-hoc networks based on multi-channel MAC protocol with TDMA is presented in [5]. In this work based on Markov chain model, two cross-layer modules are incorporated as channel quality metric and congestion-aware metric for the design of multi-channel MAC protocol.

In cross-layer optimization strategies, complexity of the algorithms and models is of utmost significance, especially for wireless systems. In [4], authors present a low-complexity cross-layer algorithm which can be employed for jointly tuning the parameters of different protocol layers by adopting simple but effective models. Their modeling is used to obtain closed-form solution to the joint optimization problem that can be computed with a limited number of operations, while providing good video quality at the decoder. The video quality in their work is measured through simulations.

In order to enhance QoS for these applications in the IEEE WLAN, numerous techniques have been designed and proposed in the literature. A QoS differentiation method is proposed in [12] for enhancing QoS over WLAN. In [13], QoS enhancement for real-time video over WLANs has been studied and an adaptive measurement-based method is proposed for allocating resources to variable bit rate video. To evaluate the performance of different QoS provisioning strategies, various analytical models based on finite and infinite queuing model are employed in the literature. In [3], the Fluid and M/G/1 models have been employed for the analysis and evaluation of its cross-layer retry-

Manuscript received October 14, 2009; revised February 26, 2010; accepted March 28, 2010. Date of publication May 18, 2010; date of current version July 16, 2010. This work was partially presented at the IEEE Wireless Communications and Networking Conference, (WCNC), 2009 [1]. The associate editor coordinating the review of this manuscript and approving it for publication was Dr. Gene Cheung.

H. Bobarshad and M. R. Shikh-Bahaei are with the Center for Telecommunication Research, King's College London, Strand, London WC2R 2LS, U.K. (e-mail: hossein.bobarshad@kcl.ac.uk; m.sbahaei@kcl.ac.uk).

M. van der Schaar is with the Electrical Engineering Department, University of California, Los Angeles, CA 90095 USA (e-mail: mihaela@ee.ucla.edu).

Digital Object Identifier 10.1109/TMM.2010.2050734

limit optimization technique, which has been proposed for enhancement of video transmission over IEEE WLANs. A definition for "packet overflow drop rate" in the M/G/1 queue analysis is provided in [3]. The use of infinite buffer size in this analysis is justified for protocols such as User Datagram Protocol (UDP) with uncontrolled source rate. In [14], the effects of wireless bandwidth variations are investigated in the case of real-time Motion Picture Experts Group (MPEG) video transmission. The MPEG encoder is controlled in order to adapt its emission rate to the current bandwidth offered by the wireless link. Switched Batch Bernoulli Process (SBBP) is employed to model both the MPEG encoder output process and the transmission-buffer service process; hence, the rather complex SBBP/SBBP/1/K queuing is used for the analysis of the queuing system. The use of finite buffer size in this work is justified due to the source rate controller in their model. Back-off time mechanism in IEEE WLAN Distributed Coordination Function (DCF) is modeled by using Markov chain in [15] and [16].

In this paper, first we revisit and assess the Fluid-model based analysis which was hinted in [3]. The model was employed in [3] for the analysis and evaluation of its cross-layer retry limit optimization technique, which has been proposed for enhancement of video transmission over IEEE WLANs. In their optimization approach, four parameters from different OSI layers are exploited: 1) Average packet rate $(\lambda)$ for incoming video from application layer, 2) MAC layer Retry-Limit $(L_r)$, 3) Average MAC layer service rate $(\mu)$, and 4) Packet Error Rate $(P_e)$ which is affected by MAC layer collisions and wireless physical layer. The aim was to derive the optimum $L_r$ based on the other three parameters, i.e., $\lambda, \mu$, and $P_e$, in order to minimize the total packet loss rate $(p_T)$, which encompasses the packet link loss rate $(p_L)$ in the Link layer and packet overflow drop rate $(p_{\rm ov})$ in the MAC layer.[1]

In addition to analytical assessment of the fluid model for analysis of the above problem, the other main contributions of this paper can be summarized as follows. We will study the application of finite-queue M/M/1/K for modeling the above-mentioned optimization method. Subsequently, we obtain a realistic mathematical estimate of the service time in IEEE WLAN transmission. Based upon this estimate, we propose exploiting M/M/1 and M/G/1 queues for more accurate analytical modeling of the same optimization problem. Then, we will exploit our proposed mathematical modeling in revisiting the Real-Time Retry-limit Adaptation (RTRA) algorithm of [3]. Finally, the accuracy of our mathematical models will be verified through computer simulations using NS-2.

The rest of this paper is organized as follows. In Section II, we explain the system scenario as the basis for our analysis with emphasis on the concept of packet loss rate. Analytical fluid model of [3] and M/M/1/K are elaborated in Section III. In Section IV, a formulation is proposed and presented to suit the retransmission phenomenon in MAC layer of IEEE WLAN. According to this formulation, M/M/1 and M/G/1 queuing-based models are derived and used to solve the cross-layer optimization problem. In Section V, we will exploit M/M/1 model to obtain and analyze a real-time adaptation algorithm. The simulation results are given in Section VI. The paper will be concluded in Section VII.

[1]Due to retransmissions, the effective service rate relative to incoming traffic rate is reduced. Hence, overflow may occur in the queue, which would cause packet overflow dropping.

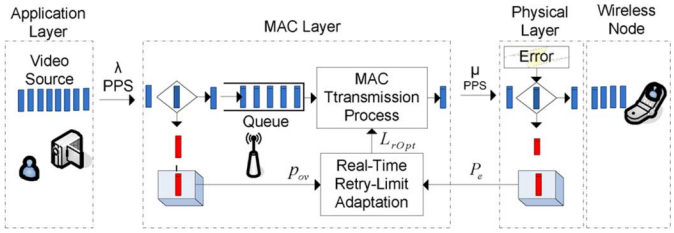


Fig. 1. Scenario used in this paper for live video communication over wireless channel.

## II. System Model

In this section, the scenario which will be studied throughout this chapter and the respective queuing system are discussed. Subsequently, a brief discussion is provided about sources of packet loss in this scenario.

### A. Scenario Description

We consider the scenario shown in Fig. 1 in which the live video packets are transmitted according to the IEEE WLAN settings. Packet loss due to the wireless time-varying channel and due to the collisions—with packets sent by other access points and nodes—is considered through the packet error rate $(P_e)$ parameter. In this scenario, UDP is used for connection between the video source and the wireless node, and packets are transmitted through a combination of wired line and wireless link. The wired link between the camera and the access point is assumed to be error-free,[2] and the wireless channel remains constant during one frame interval but varies from frame to frame, where a number of video packets constitute one frame. The access point adaptively adjusts the retry-limit on a frame-by-frame basis. In the retry-limit adaptation block, the optimum retry-limit $(L_r)$ is obtained in order to minimize the total packet loss $(p_T)$, by virtue of the fact that increasing retry-limit $(L_r)$ will decrease packet link loss rate $(p_L)$ and increases packet overflow drop rates.

### B. Queuing Model Description

We model this scenario by exploiting a queuing system. The live video source generated by camera is modeled by traffic distribution $a(x)$ with average rate $\lambda$ packets per second (PPS), and the wireless access point is viewed as a queuing system with service time distribution $b(x)$ and with an average service rate of $\mu$ PPS. In fact, $b(x)$ models the IEEE WLANs MAC block transmission process. We use UDP, which provides an unreliable connectionless delivery service using internet protocol (IP). We assume the entire arrived packet stream to be lined up in the queue, which operates in a first-input-first-output (FIFO) mode. The wireless channel behavior along with MAC-layer collisions are modeled by error rate parameter $P_e$. When the wireless channel is in "bad" condition with a high value of $P_e$,

[2]Note that packet drop occurs at the transmitter of the wireless access point not in the wired link between camera and access point.

the wireless access point will attempt to compensate for the excess packet link loss by conducting further transmissions. This will in turn increase the number of packets in the queue. Hence, newly arrived packets are likely to be dropped. In the WLAN IEEE WLANs, there is a maximum limit for the number of retransmissions, namely retry-limit that is denoted by $L_r$.

### C. Packet Loss Rate

In the above scenario, each packet may be lost either due to drop from the queue at the wireless access point or due to channel errors at the wireless link. Here we briefly explain the above sources of packet loss.

*1) Packet Link Loss Rate:* Due to the nature of wireless medium, the collisions packets may be lost through the channel. Assuming that the packet error rate due to these two factors is given by $P_e$, the probability of packet loss over the wireless channel after $L_r$ times of packet retransmission by the wireless access point, namely the "*packet link loss rate*" $(p_L)$, is given by

$$p_L = P_e^{L_r+1}. \tag{1}$$

*2) Packet Overflow Drop Rate:* When the wireless channel condition worsens or the input traffic rises, the number of packets in the queue will be increased. Hence, when the queue is full, newly arrived packets are likely to be dropped. This packet drop is known as "*packet overflow drop*" and the respective dropping rate is denoted by $p_{\rm ov}$. The precise definition of packet overflow drop rate varies from one queuing model to another, which will be discussed in Sections III and IV.

*3) Total Packet Loss Rate:* In the above scenario, each packet may be lost either due to dropping from the queue at the wireless access point with probability of $p_{\rm ov}$, or due to channel errors with probability of $p_L$, which leads to the total packet loss rate, $p_T$:

$$p_T = p_{\rm ov} + (1 - p_{\rm ov})p_L \tag{2}$$

where $p_L$ is obtained from (1). Assuming both $p_{\rm ov}$ and $p_L$ are relatively small such that the term $p_{\rm ov} \cdot p_L$ is negligible, the total packet loss rate can be approximately written as

$$p_T \cong p_{\rm ov} + p_L. \tag{3}$$

## III. Fluid and M/M/1/K Models

### A. Fluid Model-Based Analysis

In this section, we look closely into the analysis of the cross-layer optimization process based on Fluid model as suggested in [3]. According to this analysis, in the IEEE WLANs retransmission model, each packet could undergo up to $L_r$ times of retransmission from the wireless transmitter, if the packet error rate is guaranteed to be always less than $P_e$, then the number of transmissions that a given packet undergoes is a geometric random variable with mean $r$ [3]:

$$r = \frac{1 - P_e^{L_r+1}}{1 - P_e}. \tag{4}$$

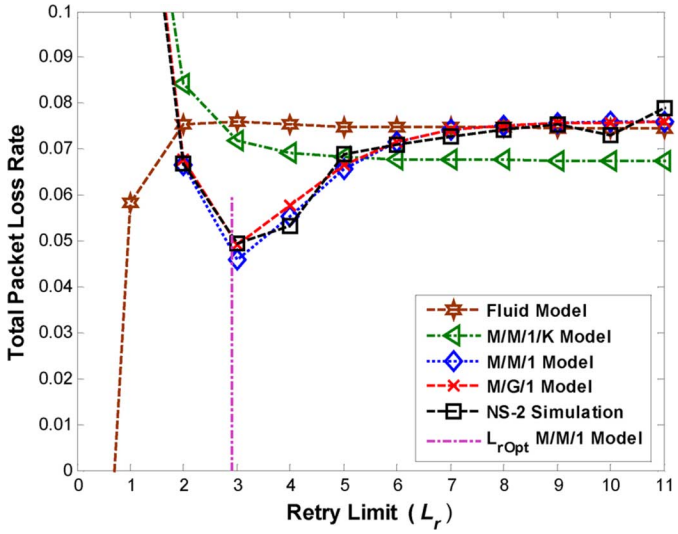


Fig. 2. Comparing total packet loss rate in Fluid, M/M/1/K, M/G/1, M/M/1 models to NS-2 simulation results when $\mu_{0_{(\rm Model)}}$ for each model is obtained from (38), $L_{\rm rM} = 11$ and other parameters are set according to Table I.

In other words, each packet is transmitted $r$ times in average from the wireless transmitter. Hence, the average processing rate $(\mu)$ is

$$\mu = \frac{\mu_0}{r} = \frac{\mu_0(1 - P_e)}{1 - P_e^{L_r+1}} \tag{5}$$

where $\mu_0$ is the processing rate of the wireless access point corresponding to $L_r = 0$ or $r = 1$, i.e., no retransmission condition. In the analysis of [3], the packet overflow drop rate $(p_{ov_{(F)}})$[3] is given as

$$p_{ov_{(F)}} = \frac{\lambda - \mu}{\lambda} \tag{6}$$

where $\mu$ is obtained from (5). Using (5) and (6) in (3) and by solving $dp_{T_{(F)}}/dL_r = 0$, the optimal retry-limit based on the Fluid model can be calculated as [3]

$$L_{r\mathrm{Opt}_{(F)}} = \log_{P_e}\left(1 - \frac{1}{\sqrt{\sigma}}\right) - 1 \tag{7}$$

where $\sigma = \lambda/\mu_0(1 - P_e)$ denotes the effective utilization factor of the link. We have shown $p_{T_{(F)}}$ versus retry-limit in Fig. 2, based on (3) wherein $p_L$ and $p_{ov_{(F)}}$ are from (1) and (6), respectively. Although simulations in [3] show that this value is close to optimal, it can be seen from Fig. 2 that the extremum for the total packet loss rate is a maximum (not minimum). This can be verified by calculating the second derivative of $p_{T_{(F)}}$ with respect to $L_r$:

$$\frac{d^2 p_{T_{(F)}}(L_r)}{dL_r^2} = \frac{-(\ln P_e)^2 P_e^{2(L_r+1)}}{1 - P_e^{L_r+1}}. \tag{8}$$

Equation (8) clearly shows that $d^2 p_{T_{(F)}}(L_r)/dL_r^2$ is always negative; hence, the value of $L_{rOpt_{(F)}}$ from (7) will maximize

[3]Note that the index (F) shows that the corresponding variable is associated with the Fluid model. In the rest of this paper, we use index (K) for the variables in M/M/1/K model, (M) for the variables in M/M/1 model, (G) for those in M/G/1 model, and (S) for NS-2 simulation results.

TABLE I
PARAMETER VALUES FOR FLUID, M/M/1/K, M/G/1, M/M/1 MODELS, AND NS-2 SIMULATION

| Parameter \ Model | Fluid | M/M/1/K | M/M/1 | M/G/1 | NS-2 |
|---|---|---|---|---|---|
| $\lambda$ (PPS) | 260 | 260 | 260 | 260 | 260 |
| $\mu_{0_{(Model)}}$ (PPS) | 375 | 405 | 455.8 | 465.7 | 472 |
| Basic Rate | - | - | - | - | 2M |
| RTS Threshold | - | - | - | - | 500 |
| ShortRetryLimit | - | - | - | - | 7 |
| ($L_r + 1$): LongRetyLimit | 1-12 | 1-12 | 1-12 | 1-12 | 1-12 |
| Queue Length | - | 50 | 50 | 50 | 50 |
| Packet Length | - | - | - | - | 1024 |
| $P_e$ | 0.4 | 0.4 | 0.4 | 0.4 | 0.4 |

the total packet loss rate $p_{T_{(F)}}$. Hence, the retry-limit value $(L_r)$ obtained mathematically according to the Fluid Model is not optimal. Therefore, we will aim to provide an alternate model for this cross-layer optimization problem and for representing retransmission and packet overflow behavior in IEEE WLANs MAC layer.

### B. M/M/1/K Model-Based Analysis

We denote $N$ as the number of packets in the finite queue of length $K$. Packet dropping probability $p_{ov_{(K)}}$ is defined as

$$p_{ov_{(K)}} = \Pr\{N = K\}. \tag{9}$$

That is, $p_{ov_{(K)}}$ is equal to the probability of having $K$ packets in the queue with length of $K$. If the service time distribution is modeled by exponential distribution with mean $1/\mu$ seconds, $p_{ov_{(K)}}$ can be approximated by [17]–[19]

$$p_{ov_{(K)}} = \frac{(1-\rho)\rho^K}{1-\rho^{K+1}} \tag{10}$$

where $\rho$ is found from solution of the following equation:

$$\begin{aligned}\rho &= \mathcal{L}\{f(x)\}_{[s=(1-\rho)\mu]} \\ &= \int_0^\infty a(x)e^{-(1-\rho)\mu x}dx.\end{aligned} \tag{11}$$

RHS of the above equation is the Laplace transform of the probability density function (pdf) of the packet inter-arrival time process, $a(x)$, at $s = (1-\rho)\mu$. Knowing that the packet inter-arrival time in M/M/1/K model has exponential pdf, $\rho$ can be obtained from (11) as

$$\rho = \frac{\lambda}{\mu} \tag{12}$$

where $\mu$ is obtained from (5). Now, having derived the packet overflow rate for M/M/1/K model, we plot $p_{T_{(K)}}$ from (3) wherein $p_{ov_{(K)}}$ and $p_L$ are from (10) and (1), respectively, in Fig. 2. As it can be seen, the minimum of $p_{T_{(K)}}$ takes place at infinity. This can be explained by examining the incoming packet rate in M/M/1/K mathematical model:

$$\lambda_k = \begin{cases} \lambda & k < K \\ 0 & k \geq K \end{cases} \tag{13}$$

*"in which the Poisson input is effectively turned off as soon as the system fills up"* [20, Ch. 3]. However, this is not practically true, as video source rate is not practically controlled by the MAC layer queue dynamics in video transmission through UDP connection.

## IV. NEW MODELS BASED ON M/G/1 AND M/M/1 QUEUING

In the following sections, we begin with obtaining a realistic estimate of the service time in IEEE WLAN transmission, and then we will employ the M/M/1 and M/G/1 models for analyzing the MAC-layer retransmission process.

### A. Estimation of Service Time for IEEE WLAN Transmission Model

As mentioned before the Fluid model assumes that the packet inter-arrival time is fixed and the service time for all transmission events is constant, which is not always a realistic assumption for a system such as IEEE WLAN. In order to improve the retransmission model, we assume that the service time pdf, $b(x)$, due to packet retransmission in IEEE WLAN can be calculated as follows:

$$b(x) = \sum_{n_r=0}^{L_r} b(x \,|\, n_r)P(n_r) \tag{14}$$

where $x$ is the service time and $P(n_r)$ denotes the probability of attempting $n_r$ retransmissions of a single packet to succeed or to reach the retry-limit $L_r$. Hence, $P(n_r)$ can be written as

$$P(n_r) = \begin{cases} (1-P_e)P_e^{n_r} & (n_r < L_r) \\ P_e^{n_r} & (n_r = L_r). \end{cases} \tag{15}$$

Also denote the conditional pdf of service time, given that $n_r$ retransmissions of a single packet are performed, by $b(x|n_r)$. We assume that this conditional pdf has an exponential distribution with average service time of $(n_r+1)/\mu_0$ (seconds), where $1/\mu_0$ denotes the wireless link average service time. Therefore, we have

$$b(x \,|\, n_r) = \frac{\mu_0}{n_r+1}e^{-\frac{\mu_0}{n_r+1}x}. \tag{16}$$

For $L_r = 0$, with no retransmission, the average value of service time is equal to $1/\mu_0$ (seconds), and hence, the respective service time pdf can be written as

$$b(x \,|\, n_r = 0) = \mu_0 e^{-\mu_0 x}. \tag{17}$$

Although the exponential service time is not exact explanatory for the real behavior of the discrete random back-off timer in IEEE WLAN medium access method, nevertheless, we will show in the simulations that the above estimate provides a good

match to reality. By substituting (15) and (16) in (14), we have (see Appendix A)

$$b(x) = \mu_0 e^{-\mu_0 x} + \mu_0 \sum_{n_r=1}^{L_r} P_e^{n_r} \left( \frac{1}{n_r+1} e^{-\frac{\mu_0}{n_r+1}x} - \frac{1}{n_r} e^{-\frac{\mu_0}{n_r}x} \right). \quad (18)$$

Equation (18) will be the basis for our analytical model for IEEE WLAN transmission process.

### *B. M/G/1 Model-Based Analysis*

In this section, we will use the general expression in (18) for service time pdf in the queuing analysis. This will lead to M/G/1 queuing model which is a single-server system with Poisson distribution for the packet arrival process and general distribution for service time. In order to evaluate the packet overflow rate, a hypothetically finite buffer size $K_A$ will be invoked in our M/G/1 based mathematical modeling. Generated packets will be dubbed "overflow packets" in the event that upon arrival, they find $K_A$ packets in this hypothetical buffer. In other words, packet overflow drop rate $(p_{ov_{(G)}})$ is the probability that an arriving packet finds no room in the hypothetical queue. This is in contrast with M/M/1/K model in which the packet arriving rate $(\lambda)$ is set to zero when the buffer is full. Our model is similar to the practical case where in a waiting room, there is limited number of chairs for the customers, and any customer that upon arrival does not find a seat has to stand (see [21, Section 2.2.4]). With one packet under service, this probability can be calculated from

$$p_{ov_{(G)}} = \Pr\{N \geq K_A + 1\} = \sum_{n=K_A+1}^{\infty} p_{n_{(G)}} = 1 - \sum_{n=0}^{K_A} p_{n_{(G)}} \quad (19)$$

where $N$ is the total number of packets in the system and $p_{n_{(G)}}$ is the system state, namely the probability that there are $n$ packets in the system. In Appendix B, we have shown that $p_{n_{(G)}}$ can be calculated as

$$p_{n_{(G)}} = (1-\rho) d_n \quad (20)$$

where

$$d_n = \begin{cases} a_n - \sum_{k=1}^{n} b_k d_{n-k} & (n = 1, 2, \ldots) \\ 1 & (n = 0) \end{cases}$$
$$a_n = \frac{v_n - v_{n-1}}{v_0}, \quad b_n = \begin{cases} \frac{v_n}{v_0} & n = 1 \\ \frac{v_1 - 1}{v_0} & n > 1 \end{cases} \quad (21)$$

and

$$v_n = \frac{1}{1+\rho_0} \left( \frac{\rho_0}{1+\rho_0} \right)^n + \sum_{n_r=1}^{L_r} P_e^{n_r} \left[ \frac{1}{1+\rho_0(n_r+1)} \left( \frac{\rho_0(n_r+1)}{1+\rho_0(n_r+1)} \right)^n - \frac{1}{1+\rho_0 n_r} \left( \frac{\rho_0 n_r}{1+\rho_0 n_r} \right)^n \right]. \quad (22)$$

Hence, the packet overflow drop rate can be calculated, by substituting (20) into (19), as follows:

$$p_{ov_{(G)}} = 1 - \sum_{n=0}^{K_A} (1-\rho) d_n. \quad (23)$$

Due to the complexity of the formulas in M/G/1 model, we will obtain the optimum retry limit by finding the minimum total packet loss rate from the numerical results shown in Fig. 2. In this figure, $p_{T_{(G)}}$ is obtained from (2) wherein $p_{ov_{(G)}}$ and $p_L$ are given by (23) and (1), respectively. As it can be seen, there is a minimum value for $p_{T_{(G)}}$ which takes place around $L_r = 3$ (with $\lambda = 260$ PPS, $\mu_0 = 465.7$ PPS, $P_e = 0.4$, $K_A = 50$), and can be considered as the optimal value for retry-limit $L_r$.

### *C. M/M/1 Model-Based Analysis*

Due to complexity of the M/G/1 model, we consider a simplified version of M/G/1 analysis by approximating the service time pdf in (18) with an exponential distribution as

$$\hat{b}(x) = \mu e^{-\mu x}. \quad (24)$$

In deriving the mean service time $1/\mu$ in the above approximated formula, we use the general expression for $b(x)$ in (18) (see Appendix C):

$$1/\mu = E[b(x)] = \int_0^{\infty} x b(x) dx = \frac{1}{\mu_0} \left[ \frac{1 - P_e^{L_r+1}}{1 - P_e} \right]. \quad (25)$$

From (25), $\mu$can be written as

$$\mu = \frac{\mu_0}{r} \quad \text{where } r = \frac{1 - P_e^{L_r+1}}{1 - P_e}. \quad (26)$$

With this assumption, the M/G/1 model is reduced to the M/M/1 model which is a single-server system, with Poisson-distributed arrivals and Exponential service-time distribution, with the mean arrival rate of $\lambda$ and mean service rate of $\mu$. The concept of hypothetical finite buffer size, which was exploited in our M/G/1-based analysis, can be used here for M/M/1 modeling of the transmission system. Assuming $N$ is the total number of packets in the queuing system and $p_{n_{(M)}}$ is the system state in the M/M/1 model, the packet overflow rate can be obtained as

$$p_{ov_{(M)}} = \Pr\{N \geq K_A + 1\} = \sum_{n=K_A+1}^{\infty} p_{n_{(M)}} \quad (27)$$

where $p_{n_{(M)}}$ can be obtained ([20, Ch. 3]) as

$$p_{n_{(M)}} = (1-\rho)\rho^n \quad (28)$$

where $\rho = \lambda/\mu$ and $\mu$ is given by (26). By incorporating (28) in (27), the overflow packet drop rate will be obtained as

$$p_{ov_{(M)}} = \sum_{k=K_A+1}^{\infty} (1-\rho)\rho^k = \rho^{K_A+1}. \quad (29)$$

Therefore, we have

$$p_{ov_{(M)}} = \left( \rho_0 \frac{1 - P_e^{L_r+1}}{1 - P_e} \right)^{K_A+1} \quad (30)$$

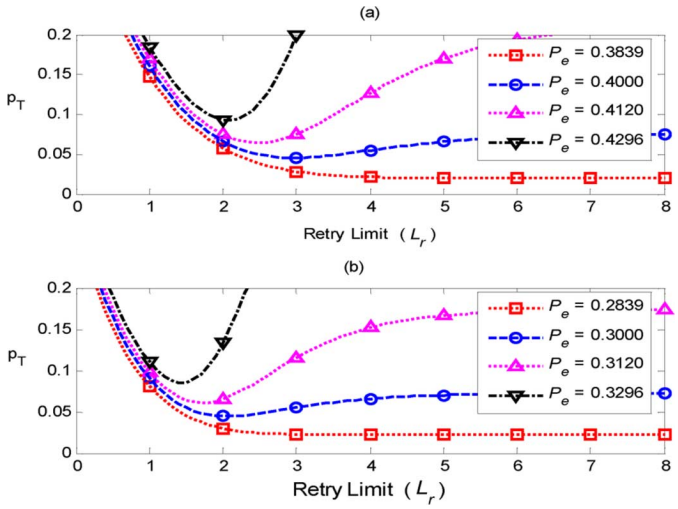


Fig. 3. Total packet loss rate versus $L_r$ for different values of $P_e$ in M/M/1-based model ($\mu_0 = 455.8$ PPS, $K_A = 50$). (a) $\lambda = 260$ PPS. (b) $\lambda = 300$ PPS.

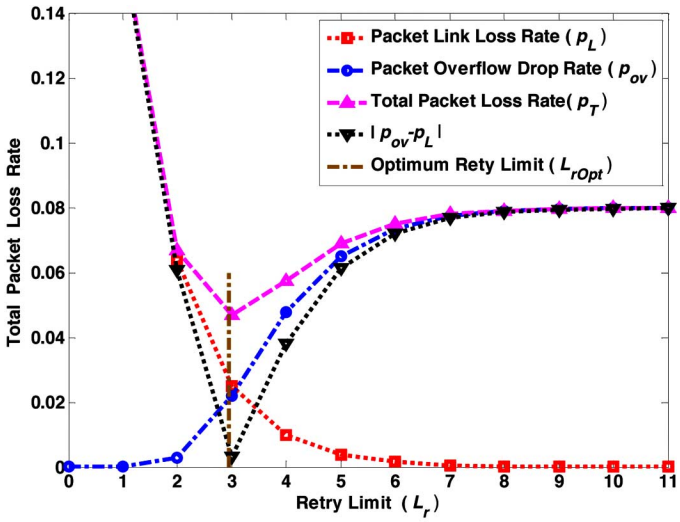


Fig. 4. $p_L, p_{ov_{(M)}}, p_T$, and $\left|p_{ov_{(M)}} - p_L\right|$ along with $L_{\mathrm{rOpt}}$ versus $L_r$, in M/M/1 model ($\lambda = 260$ PPS, $\mu_0 = 455.8$ PPS, $P_e = 0.4$).

where $\rho_0 = \lambda/\mu_0$. Total packet loss rate in M/M/1 queuing model, $p_{T_{(M)}}$, can be obtained by using (1) and (30) in (3) as

$$p_{T_{(M)}} = \left(\rho_0 \frac{1 - P_e^{L_r+1}}{1 - P_e}\right)^{K_A+1} + P_e^{L_r+1}. \tag{31}$$

Now by solving $dp_{T_{(M)}}/dL_r = 0$, the optimal $L_r$ in our M/M/1 model, $L_{rOpt_{(M)}}$, will be obtained as

$$L_{rOpt_{(M)}} = \log_{P_e}\left(1 - \frac{1 - P_e}{\rho_0}\sqrt{[K_A]\frac{1 - P_e}{(K_A + 1)\rho_0}}\right) - 1. \tag{32}$$

For $\lambda = 260$ (PPS), $\mu_0 = 455.8$ (PPS), $P_e = 0.4$, and $K_A = 50$, the optimum $L_r$ for the minimum total packet loss rate is equal to $L_{rOpt_{(M)}} = 2.9535$. $p_{T_{(M)}}$ and $L_{rOpt_{(M)}}$, from (31) and (32), respectively, are shown in Fig. 2 along with the results of the Fluid, M/M/1/K, and M/G/1 models. In this figure, $L_{rOpt_{(M)}}$ is shown by a vertical line.

## V. Retry Limit Adaptation Algorithm

In this section, we consider an algorithm for optimizing the number of retransmissions in an adaptive fashion. This is a modified version of the algorithm which is mentioned in [3] without providing an exact mathematical analysis. Our aim here is to derive the algorithm through an analytical argument and analyze it by employing the M/M/1-based model of the previous section. Subsequently, we will obtain the mathematical conditions for validity of this algorithm. We begin with considering Fig. 3, which has been obtained from the M/M/1-based analysis. From this figure, it can be seen that for a given value of $\lambda$, the optimum retry-limit corresponding to the minimum total packet loss rate varies with packet error rate $(P_e)$. Therefore, it will make sense to employ an adaptive scheme so that optimum retry-limit is dynamically changed with $P_e$. Analytical and experimental methods for estimation and measurement of PER in wireless networks, and specifically in WLAN, has been presented in the research and industrial publications, for instance [22]–[24].

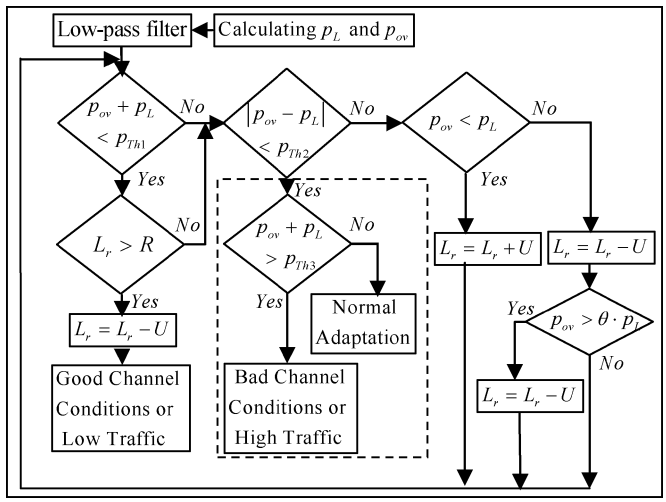


Fig. 5. Flowchart for the adaptive algorithm ($p_{Th1} = 0.02, p_{Th2} = 0.005, p_{Th3} = 0.1, \mathrm{R} = 5, \theta = 10, \mathrm{U} = 1$).

### A. Algorithm Structure

In order to visualize the logic behind the algorithm, the variation of $p_L, p_{ov_{(M)}}, p_{T_{(M)}}$, and $|p_{ov_{(M)}} - p_L|$ versus retry-limit $(L_r)$ is shown in Fig. 4 according to our M/M/1 model. We have highlighted the value of $L_{\mathrm{rOpt}}$ in this figure. From Fig. 4, it is clear that minimizing $p_{T_{(M)}}$ is tantamount to nearly having $|p_{ov_{(M)}} - p_L| = 0$. Therefore, the optimum $L_r, L_{\mathrm{rOpt}}$, approximately corresponds to the condition where $p_L$ is equal to $p_{ov_{(M)}}$. Also from the figure we note that $p_L > p_{ov_{(M)}}$ for $L_r < L_{\mathrm{rOpt}}$, and $p_L < p_{ov_{(M)}}$ for $L_r > L_{\mathrm{rOpt}}$. Based upon the above observation, the flowchart for the algorithm is given in Fig. 5. In this flowchart, a low-pass filter of the form $X_n = 0.5X_{n-1} + 0.5X_n$ is used to produce smoothed results.

### B. Algorithm Constraints

In the following, we derive the upper and lower bounds for $P_e$ according to our M/M/1-based analyses. In order to obtain a real-valued answer to $dp_{T_{(M)}}/dL_r = 0$, the following condition must be met.

*Constraint 1:* The first constraint is a direct result of inequality $\rho = (\lambda/\mu) < 1$, which is a well-known requirement in queuing theory. Using (26), we have

$$\rho = \frac{\lambda}{\mu} = \frac{\rho_0(1 - P_{\rm eH}^{L_r+1})}{1 - P_{\rm eH}} < 1 \tag{33}$$

where $\rho_0 = \lambda/\mu_0$ and $P_{\rm eH}$ is the upper-bound of $P_e$. For the case where $\rho$ is close to one, queue is in critical condition and this happens when $L_r$ is large. For large values of $L_r$ in (33), we can neglect $P_{\rm eH}^{L_r+1}$, and find the approximate upper-bound for $P_e$ as

$$P_{\rm eH} < 1 - \rho_0. \tag{34}$$

The algorithm needs checking the amount of $p_{\rm ov} + p_L$ to ensure that $p_T$ are within the desired range. Hence, in addition to comparing with threshold $p_{Th1}$, we have added a new stage—dashed line block in Fig. 5—in the algorithm of [3] where we have introduced a new threshold $p_{Th3}$. Also according to the above discussion, threshold $P_{Th2}$ is introduced for checking the value of $|p_{ov_{(M)}} - p_L|$. Also a parameter $\theta$ is used in the algorithm which effectively speeds up the convergence in case that the above difference is large. Parameter $R$ is used to avoid large delays due to large number of retransmissions.

*Constraint 2:* In order to obtain a positive real value for the optimum retry-limit in (32), we need to satisfy

$$\left(1 - \frac{1 - P_e}{\rho_0}\sqrt{[K_A]}\frac{1 - P_e}{\rho_0(K_A + 1)}\right) > 0. \tag{35}$$

Hence, we have the following lower-bound, $P_{\rm eL}$, for $P_e$:

$$P_{\rm eL} > 1 - \rho_0(K_A + 1)^{\frac{1}{K_A+1}}. \tag{36}$$

The above two constraints, (34) and (36), for M/M/1-based model can be summarized as

$$1 - \rho_0(K_A + 1)^{\frac{1}{K_A+1}} < P_e < 1 - \rho_0. \tag{37}$$

Setting $\mu_0 = 455.8$ PPS and $K_A = 50$ in (37), $P_e$ will be bounded within $0.3839 < P_e < 0.4296$ and $0.2839 < P_e < 0.3296$, respectively, for $\lambda = 260$ PPS and $\lambda = 300$ PPS. We have assessed the performance of this algorithm through simulation. $P_e$ is assumed to be a normally-distributed random value within $0.3839 < P_e < 0.4296$ and the optimum $L_r$ is obtained by exploiting the algorithm of Fig. 5 for each sample of $P_e$, which corresponds to a given channel state.[4] Numerical analysis has shown that setting $p_{Th1} = 0.02, p_{Th2} = 0.005, \mathrm{R} = 5$ and $\theta = 10$ can provide the optimal set of control parameters in the algorithm. In Fig. 6, we have compared the optimum $L_r$ derived from algorithm with the theoretical $L_{\rm rOpt}$ according to (32) over a given period of time. In Fig. 6(a), we have set $U = 0.2$, which is a theoretical value, whereas in Fig. 6(b), the step size for retry-limit, U, is set to the practical value of "one" and the value of $L_{\rm rOpt}$ from (32) is rounded to the nearest integer number.

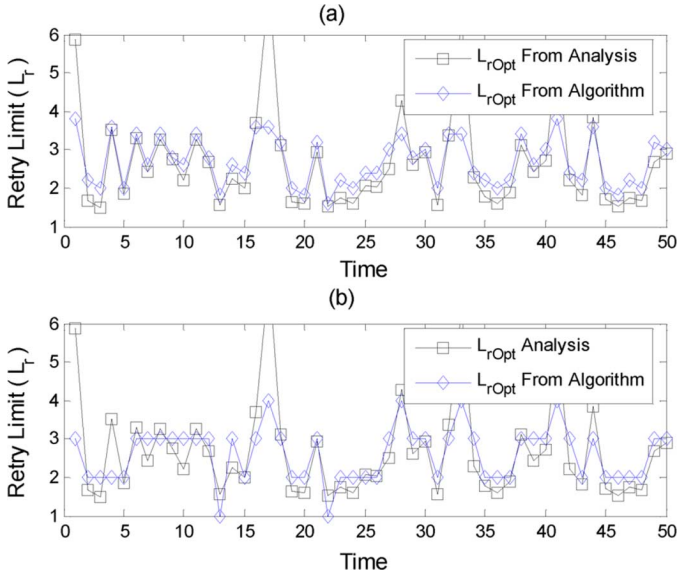


Fig. 6. Trace of retry-limit in adaptive algorithm, based on M/M/1 model. (a) $\mathrm{U} = 0.2$. (b) $\mathrm{U} = 1$.

This figure shows that our M/M/1 model-based analysis can quite precisely predict the process of retry limit adaptation in the above algorithm. Likewise, our mathematical model can be applied for evaluation of other adaptive MAC retry limit methods.

## VI. Simulations and Evaluation of the Models

### A. Poisson Traffic Simulation

We use NS-2 network simulator for simulation of the presented scenario in Fig. 1, which consists of a live video source, an access point, and a wireless node, with the parameters set as in Table I. In this simulation, the live video source is modeled by a Poisson-distributed traffic source which sends packets to the access point through a high capacity error-free wired channel. The access point forwards the traffic towards the wireless node via a typical IEEE 802.11b wireless fading channel using two-ray propagation model. The service rate in the IEEE 802.11b MAC layer is dependent on routing, transmission power, wireless physical bandwidth, and packet data rate. In order to reflect these practical parameters in our work, these are collectively considered by service rates $\mu_{0_{(Model)}}$ and $\mu_{0_{(S)}}$, respectively, for the mathematical and simulation models. In simulation, $\mu_{0_{(S)}}$ is the measured service rate of the wireless

[4]The assumption of Normal distribution for PER is not important in our simulations, as our algorithm is a function of estimated PER regardless of statistical properties of the PER variations. The simulation results corresponding to a two-state PER distribution are also shown in the following section.

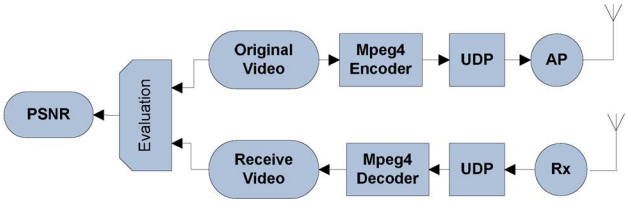


Fig. 7. Real video communication over a wireless network.

link and is set to the maximum value of packet arrival rate without incurring overflow and under no retransmission. In mathematical analysis, we have set the service rate $(\mu_{0_{(\text{Model})}})$ for each model so that the respective overflow rate is close to the simulation results. That is, $\mu_{0_{(\text{Model})}}$ for each model is obtained as follows:

$$\underset{\mu_{0_{(\text{Model})}}}{\operatorname{argmin}} \sum_{L_r=0}^{L_{\text{rM}}} \left| p_{ov_{(\text{Model})}} - p_{ov_{(S)}} \right|^2 \tag{38}$$

where $p_{ov_{(\text{Model})}}$ is one of the $p_{ov_{(F)}}, p_{ov_{(K)}}, p_{ov_{(M)}}$ or $p_{ov_{(G)}}$ and $\mu_{0_{(\text{Model})}}$ is, respectively, $\mu_{0_{(F)}}, \mu_{0_{(K)}}, \mu_{0_{(M)}}$ or $\mu_{0_{(G)}}$. The range of $L_{\text{rM}}$ and the respective values for $\mu_{0_{(\text{Model})}}$ and $\mu_{0_{(s)}}$ are presented in Table I. Dash in Table I shows that the parameter is not defined for the respective model.

We have plotted the total packet loss rate, $p_T$, for all models and for the simulation results based on the NS-2 in Fig. 2 using the parameters in Table I. In particular, the results of Fig. 2 give the optimum $L_r$ corresponding to various mathematical models, for a given instant of $P_e$. Of course, the optimum $L_r$ will vary as $P_e$ takes on a new value. It can be seen that solving the optimization problem by using M/M/1 and M/G/1 models results in a finite value for retry limit, which is in line with simulation results. The corresponding retry limit value based on M/M/1/K models tends to infinity.

According to Table I and also from Fig. 2, the M/G/1 model provides the best match to the simulation results compared to M/M/1, M/M/1/K, and Fluid models, at the expense of more complexity than the other models. The M/M/1 model, however, shows a simple and yet quite accurate model for analyzing the IEEE WLANs real-time video transmission process.

### B. Real Video Traffic Simulation

The simulation results in Sections VI-A were based on Poisson traffic, which is in line with the assumptions in M/M/1 and M/G/1 models. In this section, real video traffic source will be used for simulations in order to evaluate the applicability of the models to such cases.

The simulation set-up for real video transmission is shown in Fig. 7. First, the "Highway" video clip in Common Intermediate Format (CIF) frames was used as the video source (Fig. 8). Then the simulations were carried out with "Foreman" video clip as the source (Fig. 9).

After compressing the CIF into the MPEG4 format (see [25] for detail of the parameter settings), each video frame will be fragmented into the maximum size of 1000 bytes. Furthermore, by adding 20 bytes IP header and 8 bytes UDP header, the maximum packet size will be 1028 bytes in transmission. In the simulation results of Figs. 8 and 9, the two-state Markov model

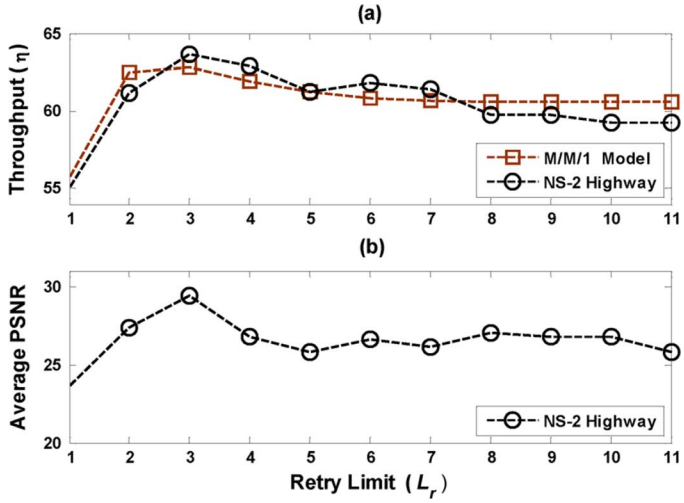


Fig. 8. Highway video clip. (a) Average throughput for various value of $L_r$ for both simulation and the M/M/1 model. (b) Average PSNR based on simulations, with $P_e = 0.45$.

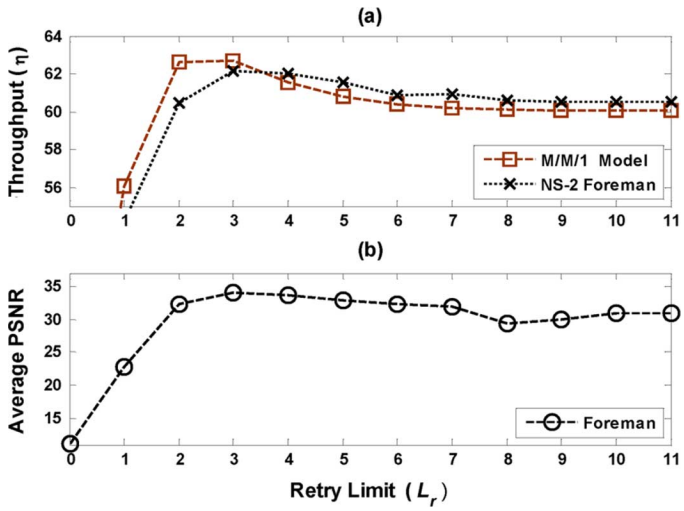


Fig. 9. Foreman video clip. (a) Average throughput for various value of $L_r$ for both simulation and the M/M/1 model. (b) Average PSNR based on simulations, with $P_e = 0.2$.

of Gilbert-Elliott error channel is used, and the parameters are set according to Table II, and $K_A = 50$. $p_{\text{NM}}$ is the transition probability from state $N$ to state $M$;$p_G$ and $p_B$ are the packet error rate in state $G$ and $B$, respectively; and $P_{e_{(GE)}}$ is the average packet error rate for Gilbert-Elliott error channel model. The state probabilities, i.e., the probability for states $G$ (Good) and $B$ (Bad), are denoted by $\pi_G$ and $\pi_B$. The NS-2 simulations were run for 12 times, each time with a different $L_r$. System throughput for the two video clips corresponding to these 12 simulations has been plotted in Figs. 8(a) and 9(a), respectively. The system throughput $(\eta)$ in this figure is given by

$$\eta = \lambda(1 - p_T). \tag{39}$$

To evaluate the application layer QoS of the video, we use the PSNR measure [26]. PSNR measures the error in the $n$th reconstructed video frame and is defined, in logarithmic scales,

TABLE II
PARAMETERS FOR FIGS. 8 AND 9

| Clip (CIF) | Frame Rate (FPS) | $\pi_G$ | $\pi_B$ | $P_{GG}$ | $P_{BB}$ | $P_{e_{(GE)}}$ |
|---|---|---|---|---|---|---|
| Highway | 30 | 0.5 | 0.5 | 0.0001 | 0.9 | 0.20 |
| Foreman | 30 | 0.5 | 0.5 | 0.0001 | 0.4 | 0.45 |

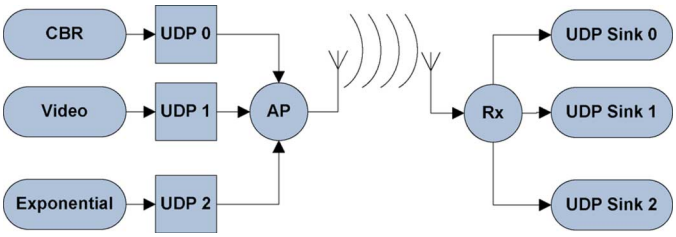


Fig. 10. NS2 simulation topology for wireless system with multiple sources.

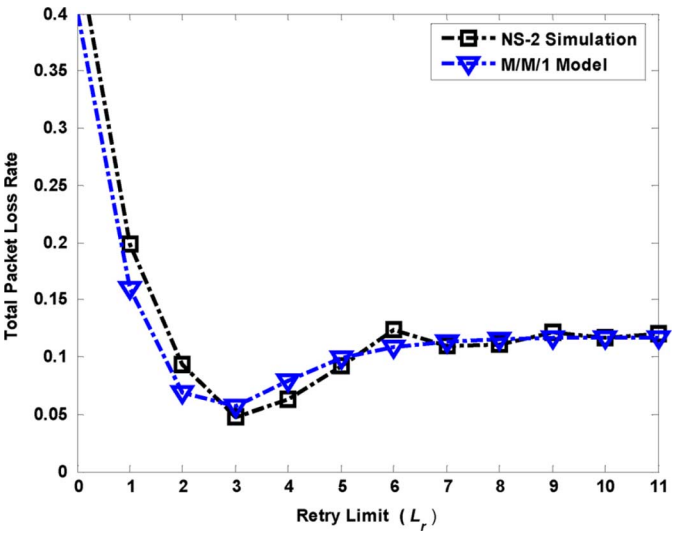


Fig. 11. M/M/1 model-based and NS-2 simulation results for wireless system with multiple sources ($\lambda = \sum_{i=1}^{\kappa} \lambda_i, P_e = 0.4, K_A = 50$).

as (40) at the bottom of the page, where luminance component (LC) is the number of bits per pixel and $N_{\text{col}} \times N_{\text{row}}$ is the display resolution which, for Common Intermediate Format (CIF) frames, is $352 \times 288$ pixels. $Y_S$ and $Y_D$ are the LC of the $n$th source and destination video frames, respectively. For calculating the parameters in the definition of PSNR, we have used Video Quality Evaluation Tool-set [27]. For each $L_r$ value, the PSNR corresponding to every frame of the "Highway" and "Foreman" video clips is calculated. Figs. 8(b) and 9(b) plot the average PSNR versus $L_r$ for "Highway" and "Forman" video clips, respectively.

As it can be seen, the average PSNR curve is maximized at $L_r = 3$.[5] In Figs. 8(a) and 9(a), the curves corresponding to M/M/1 model are given along with simulation results, which show the accuracy of the M/M/1 model for a practical arrival traffic distribution. From the results for both simulation and the M/M/1 model, it can be seen that throughput varies with $L_r$, with a maximum occurring at $L_r \cong 3$. In analyzing the simulation results, it is important to note that: 1) as for the service time in the simulations, we have employed the actual service time which is provided by Network Simulator according to WLAN IEEE 802.11. For evaluation of our models and for comparison of our theoretical results with simulations, the expressions $(b(t))$ and $(\hat{b}(t))$ are used, respectively, for service time in M/G/1 and M/M/1 based models. 2) We have used real-video as the incoming traffic for the simulation results in Figs. 8 and 9. Only in Fig. 2 is the incoming traffic Poisson-distributed, in which case the service time for simulation is again the actual service time not Exponential. Also the service times corresponding to M/G/1 and M/M/1 in Fig. 2 are, respectively, the expressions $(b(t))$ and $(\hat{b}(t))$.

In Figs. 10 and 11, the above real video simulation is repeated with two other sources, including "Poisson" and "Constant Bit Rate" (CBR) traffics. All traffics are transmitted over UDP. Poisson traffic has a data rate of 1 Mbps and its packet size is 1024 bytes. The CBR traffic data rate is 256 Kpbs and CBR packet size is 1500 bytes. The "Total packet loss rate", according to the NS-2 simulation results and for the M/M/1 model, are plotted in Fig. 11. $\lambda$ for the composite traffic can be calculated as the sum of individual arrival rates [29].

## VII. CONCLUSION AND FUTURE WORK

We investigated four different mathematical models to analyze a video QoS provisioning strategy over WLAN based on cross-layer optimization, wherein parameters in MAC, Application, and Physical layers are jointly considered. Analysis of the Fluid and M/M/1/K models revealed some deficiencies in using them for predicting the IEEE WLAN retransmission process. Subsequently, we proposed invoking two mathematical models based on M/M/1 and M/G/1 queuing and showed that these can model MAC transmission process more accurately. Using

[5]It is actually possible to enhance the PSNR by improving the codec parameters (for example, see [28]).

$$\text{PSNR}(n)_{\text{dB}} = 20\log_{10}\left(\frac{2^{\text{LC}}-1}{\frac{1}{N_{\text{col}}N_{\text{row}}}\sum_{i=0}^{N_{\text{col}}}\sum_{j=0}^{N_{\text{row}}}[Y_S(n,i,j)-Y_D(n,i,j)]^2}\right) \tag{40}$$

these models, packet overflow rate was found analytically. In particular, we have shown that M/M/1 is a fairly simple model that yields close results to M/G/1. Using our M/M/1 model, we derived closed-form expressions for the packet overflow drop rate and the optimal retry limit, and showed that our M/M/1 queuing-based model can be efficiently applied in order to evaluate adaptive retry-limit algorithms in IEEE WLANs. Finally, we confirmed the accuracy of our mathematical models through computer simulations (NS2).

In the follow-up investigation to this work, our adaptive scheme will be studied in the case where delay constraint is also present. We will analyze that scenario by introducing an "expired-time packet discard rate". We have shown in [29] that for delay-limited applications, there is a trade-off between overflow packet drop rate and expired-time discard rate.

## APPENDIX

### *Appendix A*

Deriving (18): By expanding (14) and substituting (15) and (16) in it, we have

$$\begin{aligned} b(x) = {} & \mu_0 e^{-\mu_0 x}(1-P_e) + \frac{\mu_0}{2} e^{-\frac{\mu_0}{2}x}(1-P_e)P_e \\ & + \frac{\mu_0}{3} e^{-\frac{\mu_0}{3}x}(1-P_e)P_e^2 + \cdots \\ & + \frac{\mu_0}{L_r} e^{-\frac{\mu_0}{L_r}x}(1-P_e)P_e^{L_r-1} + \frac{\mu_0}{L_r+1} e^{-\frac{\mu_0}{L_r+1}x} P_e^{L_r}. \end{aligned} \tag{A1}$$

Expanding and regrouping the terms in (A1), we have

$$\begin{aligned} b(x) = {} & \mu_0 e^{-\mu_0 x} + P_e\left(\frac{\mu_0}{2} e^{-\frac{\mu_0}{2}x} - \mu_0 e^{-\mu_0 x}\right) \\ & + P_e^2\left(\frac{\mu_0}{3} e^{-\frac{\mu_0}{3}x} - \frac{\mu_0}{2} e^{-\frac{\mu_0}{2}x}\right) \\ & + P_e^3\left(\frac{\mu_0}{4} e^{-\frac{\mu_0}{4}x} - \frac{\mu_0}{3} e^{-\frac{\mu_0}{3}x}\right) \\ & \vdots \\ & + P_e^{L_r-1}\left(\frac{\mu_0}{L_r} e^{-\frac{\mu_0}{L_r}x} - \frac{\mu_0}{L_r-1} e^{-\frac{\mu_0}{L_r-1}x}\right) \\ & + P_e^{L_r}\left(\frac{\mu_0}{L_r+1} e^{-\frac{\mu_0}{L_r+1}x} - \frac{\mu_0}{L_r} e^{-\frac{\mu_0}{L_r}x}\right). \end{aligned} \tag{A2}$$

Equation (A2) can be written as

$$\begin{aligned} b(x) = {} & \mu_0 e^{-\mu_0 x} + \mu_0 \sum_{n_r=1}^{L_r} P_e^{n_r} \\ & \times \left(\frac{1}{n_r+1} e^{-\frac{\mu_0}{n_r+1}x} - \frac{1}{n_r} e^{-\frac{\mu_0}{n_r}x}\right). \end{aligned} \tag{A3}$$

### *Appendix B*

In this Appendix, we aim to find the probability that there are $n$ packets in our M/G/1 queuing system, $p_{n_{(G)}}$. According to [20, Ch. 5], this probability is identical to the probability that there are $n$ packets in M/G/1 queuing system at the departure instants, $q_{n_{(G)}}$. Hence, according to the notations of [20, Ch. 5], we derive $q_{n_{(G)}}$ for our M/G/1 model as follows. The generating function of $q_{n_{(G)}}, Q(z)$ in [20, Ch. 5] is given as

$$\begin{aligned} Q(z) = B^*(\lambda - \lambda z)\frac{(1-\rho)(1-z)}{B^*(\lambda-\lambda z) - z}, \\ \text{where } B^*(s) = \textstyle\int_0^\infty e^{-sx} b(x)\, dx. \end{aligned} \tag{B4}$$

Hence, for $B^*(\lambda - \lambda z)$, which is denoted by $V(z)$. we have

$$V(z) = B^*(\lambda - \lambda z) = \int_0^\infty e^{-(\lambda - z\lambda)x} b(x) dx. \tag{B5}$$

By substituting $b(x)$ from (18) into (B5), we have

$$\begin{aligned} V(z) = {} & \frac{\mu_0}{\lambda - z\lambda + \mu_0} + \sum_{n_r=1}^{L_r} P_e^{n_r}\left[\frac{1}{n_r+1}\right. \\ & \left. \times \left(\frac{\mu_0}{\lambda - z\lambda + \frac{\mu_0}{n_r+1}}\right) - \frac{1}{n_r}\left(\frac{\mu_0}{\lambda - z\lambda + \frac{\mu_0}{n_r}}\right)\right]. \end{aligned} \tag{B6}$$

Noting that $\rho_0 = \lambda/\mu_0$, we have

$$\begin{aligned} V(z) = {} & \frac{\frac{1}{1+\rho_0}}{1 - \frac{\rho_0}{1+\rho_0} z} + \sum_{n_r=1}^{L_r} P_e^{n_r} \\ & \times \left(\frac{\frac{1}{1+\rho_0(n_r+1)}}{1 - \frac{\rho_0(n_r+1)}{1+\rho_0(n_r+1)} z} - \frac{\frac{1}{1+n_r\rho_0}}{1 - \frac{n_r\rho_0}{1+n_r\rho_0} z}\right). \end{aligned} \tag{B7}$$

Deploying geometric series expansion to each term of (B7), $V(z)$ can be written as

$$\begin{aligned} V(z) = {} & \frac{1}{1+\rho_0} \sum_{n=0}^{\infty} \left(\frac{\rho_0}{1+\rho_0}\right)^n z^n \\ & + \sum_{n_r=1}^{L_r} P_e^{n_r}\left[\frac{1}{1+\rho_0(n_r+1)}\right. \\ & \times \sum_{n=0}^{\infty}\left(\frac{\rho_0(n_r+1)}{1+\rho_0(n_r+1)}\right)^n z^n \\ & \left. - \frac{1}{1+\rho_0 n_r} \sum_{n=0}^{\infty}\left(\frac{\rho_0 n_r}{1+\rho_0 n_r}\right)^n z^n\right]. \end{aligned} \tag{B.8}$$

Hence, see (B9) at the bottom of the page.

$$V(z) = \sum_{n=0}^{\infty} \left\{ \begin{array}{l} \frac{1}{1+\rho_0}\left(\frac{\rho_0}{1+\rho_0}\right)^n \\ + \sum_{n_r=1}^{L_r} P_e^{n_r}\left[\frac{1}{1+\rho_0(n_r+1)}\left(\frac{\rho_0(n_r+1)}{1+\rho_0(n_r+1)}\right)^n - \frac{1}{1+\rho_0 n_r}\left(\frac{\rho_0 n_r}{1+\rho_0 n_r}\right)^n\right] \end{array} \right\} z^n \tag{B9}$$

If we assume that $V(z)$ is the $z$ transform of $v_n$, we can write $V(z)=\sum_{n=0}^{\infty} v_n z^n$; hence, we have

$$v_n=\frac{1}{1+\rho_0}\left(\frac{\rho_0}{1+\rho_0}\right)^n + \sum_{n_r=1}^{L_r} P_e^{n_r}\left[\frac{1}{1+\rho_0(n_r+1)}\left(\frac{\rho_0(n_r+1)}{1+\rho_0(n_r+1)}\right)^n - \frac{1}{1+\rho_0 n_r}\left(\frac{\rho_0 n_r}{1+\rho_0 n_r}\right)^n\right]. \tag{B10}$$

Noting that $V(z)=B^*(\lambda-\lambda z)$ and by using (B9) in (B4), we have

$$Q(z)=\frac{(1-\rho)\left[V(z)-zV(z)\right]}{V(z)-z} = \frac{(1-\rho)\left[\sum_{n=0}^{\infty} v_n z^n - z\sum_{n=0}^{\infty} v_n z^n\right]}{\sum_{n=0}^{\infty} v_n z^n - z} \tag{B11}$$

$$Q(z)=\frac{(1-\rho)\left[v_0+\sum_{n=1}^{\infty} v_n z^n - \sum_{n=1}^{\infty} v_{n-1} z^n\right]}{v_0+(v_1-1)z+\sum_{n=2}^{\infty} v_n z^n} = (1-\rho)\frac{1+\sum_{n=1}^{\infty}\frac{v_n-v_{n-1}}{v_0}z^n}{1+\frac{v_1-1}{v_0}z+\sum_{n=2}^{\infty}\frac{v_n}{v_0}z^n} \tag{B12}$$

$$Q(z)=(1-\rho)\frac{1+\sum_{n=1}^{\infty} a_n z^n}{1+\sum_{n=1}^{\infty} b_n z^n} \quad \text{where}$$

$$a_n=\frac{v_n-v_{n-1}}{v_0},$$

$$b_n=\begin{cases}\frac{v_n}{v_0} & n=1\\ \frac{v_1-1}{v_0} & n>1.\end{cases} \tag{B13}$$

Also it can be verified by long division that $Q(z)$ can be written as

$$Q(z)=(1-\rho)\sum_{n=0}^{\infty} d_n z^n, \quad \text{where}$$

$$d_n=\begin{cases} a_n-\sum_{k=1}^{n} b_k d_{n-k} & (n=1,2,\ldots)\\ 1 & (n=0).\end{cases} \tag{B14}$$

Hence, the inverse Laplace transform of (B14) is

$$p_{n_{(G)}}=q_{n_{(G)}}=(1-\rho)d_n. \tag{B.15}$$

## *Appendix C*

Here we aim to calculate the mean value for pdf service time $b(x)$ in (18) which can be derived as

$$1/\mu=E[b(x)]=\int_0^{\infty} x b(x)dx=\int_0^{\infty}\Big[\mu_0 x e^{-\mu_0 x} + \sum_{n_r=1}^{L_r} P_e^{n_r}\left(\frac{\mu_0 t}{n_r+1}e^{-\frac{\mu_0}{n_r+1}x}-\frac{\mu_0 t}{n_r}e^{-\frac{\mu_0}{n_r}x}\right)\Big]dx. \tag{C16}$$

Knowing that $\int_0^{\infty}\mu_{n_r} x e^{-\mu_{n_r}x}dx=(1/\mu_{n_r})$, we have

$$1/\mu=\frac{1}{\mu_0}+\sum_{n_r=1}^{L_r} P_e^{n_r}\left[\frac{n_r+1}{\mu_0}-\frac{n_r}{\mu_0}\right] = \frac{1}{\mu_0}\left[1+P_e+P_e^2+P_e^3+\cdots+P_e^{L_r}\right] = \frac{1}{\mu_0}\left[\frac{1-P_e^{L_r+1}}{1-P_e}\right]. \tag{C17}$$

## REFERENCES


[1] H. Bobarshad and M. Shikh-Bahaei, "M/M/1 queuing model for adaptive cross-layer error protection in WLANs," in *Proc. IEEE Wireless Communications and Networking Conf. (WCNC)*, Apr. 2009, pp. 1–6.

[2] *Wireless LAN Medium Access Control (MAC) and Physical Layer (PHY) Specifications*, IEEE Std. 802.11-1999, 1999.

[3] Q. Li and M. Van der Schaar, "Providing adaptive QoS to layered video over wireless local area networks through real-time retry limit adaptation," *IEEE Trans. Multimedia*, vol. 6, no. 2, pp. 278–290, Apr. 2004.

[4] S. Milani and G. Calvagno, "A low-complexity cross-layer optimization algorithm for video communication over wireless networks," *IEEE Trans. Multimedia*, vol. 11, no. 5, pp. 810–821, Aug. 2009.

[5] B. J. Oh and C. W. Chen, "A cross-layer approach to multichannel MAC protocol design for video streaming over wireless ad hoc networks," *IEEE Trans. Multimedia*, vol. 11, no. 6, pp. 1052–1061, Oct. 2009.

[6] M. van der Schaar, Y. Andreopoulos, and H. Zhiping, "Optimized scalable video streaming over IEEE 802.11 a/e HCCA wireless networks under delay constraints," *IEEE Trans. Mobile Comput.*, vol. 5, no. 6, pp. 755–768, Jun. 2006.

[7] M. van der Schaar and D. S. Turaga, "Cross-layer packetization and retransmission strategies for delay-sensitive wireless multimedia transmission," *IEEE Trans. Multimedia*, vol. 9, no. 1, pp. 185–197, Jan. 2007.

[8] M. van der Schaar, D. S. Turaga, and W. Raymond, "Classification-based system for cross-layer optimized wireless video transmission," *IEEE Trans. Multimedia*, vol. 8, no. 5, pp. 1082–1095, Oct. 2006.

[9] M. van der Schaar and N. Sai Shankar, "Cross-layer wireless multimedia transmission: Challenges, principles, and new paradigms," *IEEE Wireless Commun. Mag.*, vol. 12, no. 4, pp. 50–58, Aug. 2005.

[10] Y. C. Lai, A. Chang, and J. Liang, "Provision of proportional delay differentiation in wireless LAN using a cross-layer fine-tuning scheduling scheme," *IET Commun.*, vol. 1, no. 5, pp. 880–886, 2007.

[11] N. S. Shankar and M. van der Schaar, "Performance analysis of video transmission over IEEE 802.11a/e WLANs," *IEEE Trans. Veh. Technol.*, vol. 56, no. 4, pp. 2346–2362, Jul. 2007.

[12] L. Zhao, J. Y. Wu, H. Zhang, and J. Zhang, "Integrated quality-of-service differentiation over IEEE 802.11 wireless LANs," *IET Commun.*, vol. 2, no. 2, pp. 329–335, 2008.

[13] W.-K. Kuo, "Traffic scheduling for multimedia transmission over IEEE 802.11e wireless LAN," *IET Commun.*, vol. 2, no. 1, pp. 92–97, 2008.

[14] L. Galluccio, G. Morabito, and G. Schembra, "Transmission of adaptive MPEG video over time-varying wireless channels: Modelling and performance evaluation," *IEEE Trans. Wireless Commun.*, vol. 4, no. 6, pp. 2777–2788, Nov. 2005.

[15] G. Bianchi, "Performance analysis of the IEEE 802.11 distributed coordination function," *IEEE J. Select. Areas Commun.*, vol. 18, no. 3, pp. 535–547, Mar. 2000.

[16] P. Chatzimisios, A. C. Boucouvalas, and V. Vitsas, "IEEE 802.11 packet delay—A finite retry-limit analysis," in *Proc. IEEE Global Telecommunications Conf.*, 2003, vol. 2, pp. 950–954.
[17] D. D. Kouvatsos, "Mem for arbitrary queuing networks with multiple general servers and repetitive service blocking," *Perform. Eval.*, vol. 10, pp. 169–195, 1989.
[18] R. Nagarajan, J. F. Kurose, and D. Towsley, "Approximation techniques for computing packet loss in finite buffered voice multiplexes," *IEEE J. Select. Areas Commun.*, vol. 9, no. 3, pp. 368–377, Apr. 1991.
[19] H. T. Kaur, T. Ye, S. Kalyanaraman, and K. S. Vastola, "Minimizing packet loss by optimizing OSPF weights using online simulation," in *Proc. 11th IEEE/ACM Int. Symp. Modeling, Analysis and Simulation of Computer Telecommunications Systems*, Oct. 2003, pp. 79–86.
[20] L. Kleinrock, *Queueing Systems Volume 1: Theory*. New York: Wiley-Interscience, 1975.
[21] D. Gross and C. M. Harris, *Fundamentals of Queueing Theory*, 3rd ed. New York: Wiley, 1998.
[22] B. Han and S. Lee, "Efficient packet error rate estimation in wireless networks," in *Proc. IEEE TridentCom*, May 2007, pp. 1–9.
[23] Rohde and Schwarz, 802.11 Packet Error Rate Testing—Hardware Implementation. [Online]. Available: http://www2.rohdeschwarz.com/file1344/1GP56 2E.pdf.
[24] R. Khalili and K. Salamatian, "Evaluation of packet error rate in wireless networks," in *Proc. IEEE Int. Symp. Modeling, Analysis and Simulation of Wireless and Mobile Systems, ACM MSWIM*, 2004.
[25] The Work Prepare for Multimedia Experiment. [Online]. Available: http://140.116.72.80/~jhlin5/-ns2/Prepare%20work%20for%20multimedia%20experiment.htm.
[26] How to Evaluate MPEG Video Transmission Using the NS2 Simulator. [Online]. Available: http://140.116.72.80-/~smallko/ns2/Evalvid_in_NS2.htm. available at:
[27] EvalVid—A Video Quality Evaluation Tool-set. [Online]. Available: http://www.tkn.tu-berlin.de/research/evalvid/.
[28] B. Pathak, G. Childs, and M. Ali, "Video quality enhancements with implementation of NEWPRED method for MPEG-4 over simulated UMTS channel propagation environments," *Int. J. Comput. Netw. Security (IJCNS)*, vol. 2, no. 1, pp. 70–75, Jan. 2010.
[29] H. Bobarshad, "Evaluation and modeling of real time video transmission over WLAN" Ph.D. dissertation, King's College London, London, U.K., 2010. [Online]. Available: https://cms.kcl.ac.uk/content/1/c4/17/13/ThesisHosseinBobarshad.pdf.

**Hossein Bobarshad** (S'08–GS'10) received the M.Sc. degree in communication engineering from the Iran University of Science & Technology (IUST), Tehran, Iran, and the Ph.D. degree in telecommunications from the Electronic Engineering Department of King's College London, London, U.K., in 2010.

He currently is a research assistant at King's College London. His main research interests are in the areas of data communication theory, mathematical modelling, and real time video transmission through unreliable media, e.g., wireless networks and the Internet. In particular, he conducts his research mainly on cross-layer design for adaptive error protection in video over WLAN and wireless sensor networks for monitoring of physiological signals.

**Mihaela van der Schaar** (F'10) is currently an Associate Professor in the Electrical Engineering Department at the University of California, Los Angeles. Her research interests are in multimedia communications, networking, processing and systems and, more recently, on learning and games in engineering systems.

Prof. van der Schaar received in 2004 the NSF Career Award; in 2005 the Best Paper Award from IEEE TRANSACTIONS ON CIRCUITS AND SYSTEMS FOR VIDEO TECHNOLOGY; in 2006 the Okawa Foundation Award; in 2005, 2007, and 2008 the IBM Faculty Award; and in 2006 the Most Cited Paper Award from *EURASIP: Image Communications* journal. She was an associate editor for IEEE TRANSACTIONS ON MULTIMEDIA, IEEE SIGNAL PROCESSING LETTERS, IEEE TRANSACTIONS ON CIRCUITS AND SYSTEMS FOR VIDEO TECHNOLOGY, *Signal Processing Magazine*, etc. She holds 33 granted U.S. patents and three ISO awards for her contributions to the MPEG video compression and streaming international standardization activities.

**Mohammad R. Shikh-Bahaei** (SM'08) received the B.Sc. degree in electrical engineering from the University of Tehran, Tehran, Iran, the M.Sc. degree in electronic engineering from Sharif University of Technology, Tehran, and the Ph.D. degree in wireless communications from King's College London, London, U.K., in 2000.

He has worked for Algorex Ltd., U.K. (now part of National Semiconductor Corp., California and for a start-up company, MobilSoft Ltd., U.K. In December 2000, he joined National Semiconductor Corp. (NSC), CA, USA, and worked on the design of 3rd-generation handsets based on UMTS standards, for which he has been awarded three US patents as inventor and co-inventor, respectively. He returned to the U.K. in 2002 as an academic in the Electronic Department at King's College London, where he is now an academic member of the center for telecommunication research (CTR) within the Department of Informatics. The main focus of his research has been on the analysis and design of adaptive transmitters and resource allocation techniques in wireless communications, and optimization of wireless network performance for services such as VoIP and Video-over-IP.

Dr. Shikh-Bahaei is the Lead Editor of a Special Issue of *EURASIP Journal on Wireless Communications and Networking*. He is also the founder and organizer of the annual international conference Wireless Advanced (formerly known as SPWC) which is supported by CTR of King's College London.